

In Situ Observation of Reactions at Liquid/Metal Interfaces

Masao Kimura

Adv. Tech. Res. Lab., Nippon Steel Corp., Futtsu, Chiba, 293-8511, Japan

Fax: 81-439-80-2746, e-mail: kimura@re.nsc.co.jp

In situ techniques have been developed for observation of reactions at liquid/metal interfaces. Special attention was paid to monitor the change in structures of: (a) ions and/or colloids in solutions and (b) metal surface and/or films formed on it. Pitting and atmospheric corrosion of steel were studied using these techniques in order to develop new alloy.

(1) **Pitting:** States of ions in various solutions near the interface were investigated by XAFS (X-ray Absorption Fine Structures) using a special electrochemical cell. *In situ* observation has shown the change of structures of chromium and bromine near the interface of 1M LiBr solution and Fe-18Cr-12Ni-2Mo (mass%) alloy, indicating the formation of hydrobromo-complex near the metal/solution interface. (2) **Atmospheric corrosion:** Nano-scale structures of rusts formed on the weathering steel surface were investigated quantitatively by a combination of XAFS analysis including *in situ* observation under wet conditions, X-ray diffraction (XRD), and transmission electron microscopy (TEM). It has been shown that the key structure of high corrosion-resistance is an $\text{Fe}(\text{O},\text{OH})_6$ network, which is different from crystalline FeOOH .

Key words: XAFS, corrosion, steel, wet, network

1. INTRODUCTION

Loss relating with steel corrosion is estimated to be more than a few percentage of GNP. Steel used without coating has been strongly required not only from its low costs but also from the viewpoint of life-cycle assessments of materials. Corrosion mechanism has been investigated mainly by electrochemical methods and micro-structural observation before and after corrosion.

However, there has been little information on real reactions which progress under water. In atomic scale, corrosion is a reaction that occurs at the interface of liquid and metal surface (Fig.1). *In situ* observation of reactions at liquid/metal interfaces is quite essential to understand the mechanism of corrosion and develop new alloy. In this study, *in situ* techniques have been developed and applied in order to reveal the corrosion mechanism of pitting and atmospheric corrosion.

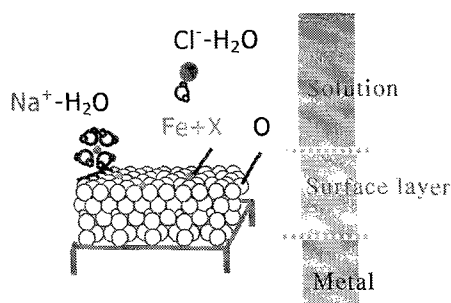


Fig.1 Schematic diagram of the liquid/metal interface in corrosion

2. EXPERIMENTS

2.1 *In situ* XAFS of ions near the interface

Figure 2 shows an electrochemical cell developed for *in situ* XAFS (X-ray Absorption Fine Structures) [1]. A sheet of stainless steel (Fe-16.8Cr-12.0Ni-2.0Mo in mass%) is attached below a reservoir of 1M LiBr solution acting as an aqueous environment. LiBr was used instead of NaCl because of a limitation of edge-energies. A specimen and the reservoir are joined by a Kapton® film; in other words, the liquid "film" joins the reservoir and a metal edge.

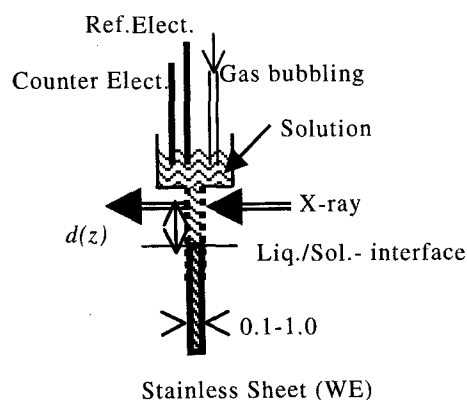


Fig.2 Schematic illustration of a newly designed electrochemical cell conducted for *in situ* XAFS measurements.

A potential of the steel was controlled by a potentiostat at 0.8V vs. Ag/AgCl reference electrode to corrode entire cross-section of the sample uniformly. After

dissolution of the sheet, the depth of the crevice reached a few mm; XAFS measurements were then carried out by transmission geometry at different positions of $d(z)$ from the dissolving interface to the bulk solution. XAFS measurements were performed at beam lines BL-7C and BL-12C [2, 3] at the Photon Factory (PF), KEK, Tsukuba, Japan.

2.2 In situ X-ray diffraction of films formed near the interface

Rust formation at an early stage of corrosion was investigated by *in situ* measurements. Surface diffractometer ("EVA" system [4]) was developed. A 2θ - θ goniometer (" χ -axis") was mounted on the θ table of another 2θ - θ goniometer (" θ -axis"). The combination of two diffractometer can be tilted against the X-ray beam from SR, which determines the angle of incidence into the surface.

Artificial seawater was used as liquid for corrosion, and the potential of the specimen was changed from -0.6 to 1.0 V vs. Ag/AgCl in a period of 1 hour. During corrosion, scattering intensities were measured using an image plate. Measurements were carried out at BL-3A at PF. A typical parameters are: the energy of X-ray = 12.399 keV and the beam size = $1 \times 1 \text{ mm}^2$.

Rust formation at a late stage of corrosion was investigated also by XAFS, XRD and TEM. XAFS measurements were carried out at BL-12C at PF.

Conventional mild steel (MS) and weathering steel (WS) was prepared as specimens. The compositions are: MS = Fe-0.60Mn-0.020P-0.30Si-0.15C and WS = Fe-0.28Cu-0.55Cr-0.15Ni-0.49Mn-0.081P-0.51Si-0.10C (in mass%).

3. RESULTS AND DISCUSSION

3.1 Pitting

Ion concentrations in the pit were investigated by *in situ* measurements of absorption at the edges. It was clearly seen that the concentrations of chromium and bromine are linearly dependent on the distance $d(z)$, suggesting that the dissolution rate can be determined by diffusion of ions.

In situ XAFS measurements of chromium and bromine ions were carried out at different positions $d(z)$, from positions near the dissolving interface and near the bulk solution. Figure 3 shows the Fourier transforms of Cr and Br K-edges spectra at different $d(z)$ positions. It was found that Cr edge spectra for all $d(z)$ positions showed peaks at almost the same position located between the Cr-Br of CrBr_3 powder and the Cr-O of Cr(OH)_3 powder.

In contrast with the spectra of chromium, Br-K edge spectra differ at different $d(z)$ position. The peak shifts toward a larger R as the distance $d(z)$ increases.

Each spectrum was analyzed by the "REX" program (Rigaku Co.), and structures around Cr and Br were analyzed. Based on these results and electrochemical consideration of the reaction, the change of complex structure inside the pit was revealed [1]. Figure 4 shows a schematic illustration of change of ion-complex structures inside the artificial crevice suggested by this study.

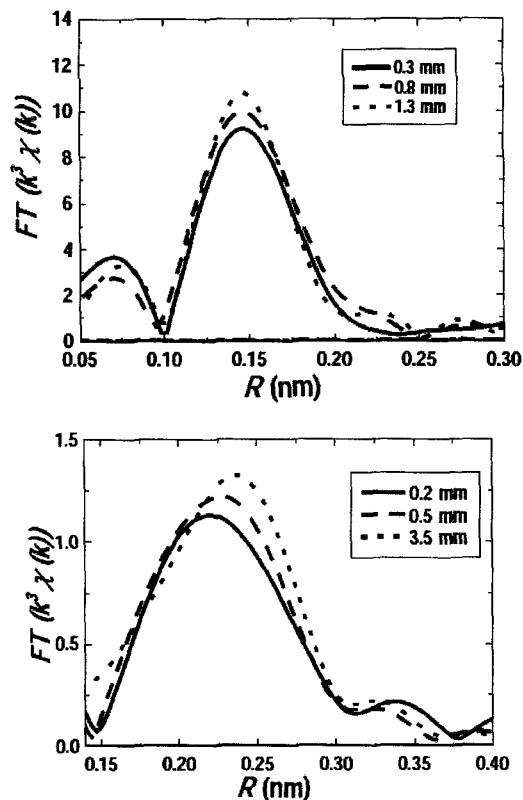


Fig.3 Fourier transforms of XAFS spectra at Cr (above) and Br (below) K-edges for different $d(z)$.

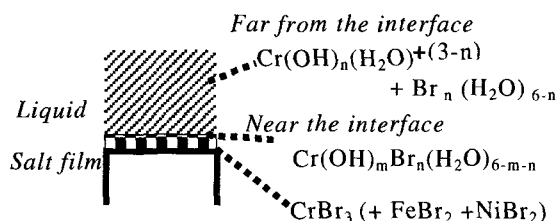
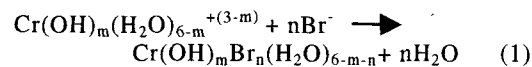


Fig.4 Schematic illustration of change of ion-complex structures inside the pit.

Far from the interface, chromium forms hydroxo complex, and bromine is simply hydrated. However, near the interface, metal ions ($M = \text{Fe, Cr, Ni}$) are expected to form hydro-bromo complex (Eq.(1)). This is why Fourier transforms change among different $d(z)$ only in Br K-edges.

These results are consistent with X-ray fluorescence measurements inside the similar pit [5, 6]. The formation of complex explains why observed values of pH were lower than the ones calculated by simple hydrolysis reaction of metal salts (Eq.(2)).



3.2 Atmospheric corrosion

During atmospheric corrosion, metals experience cycles of wet and dry. The first process of corrosion under wet conditions was measured by *in situ* observation. Figure 5 shows scattering intensities at (a) 23 min. and (b) 55 min. after the potential was applied. Diffuse intensities in Fig.5(a) correspond to an Fe(OH)_x phase: the colloidal products formed at the first stage of corrosion. Quantitative analysis has shown the diffraction peaks in Fig.5(b) correspond to the $\gamma\text{-FeOOH}$ type structure.

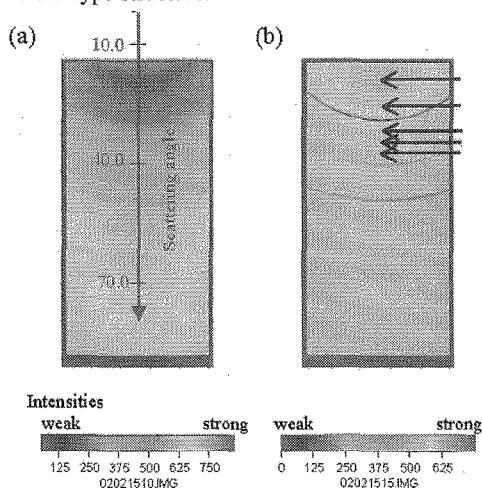


Fig.5 Scattering intensities measured by image plates at (a) 23 min. and (b) 55 min. after corrosion starts. Arrows in (b) show the peaks corresponding the $\gamma\text{-FeOOH}$ type structure.

Fe and Cr K-edges XAFS spectra were also measured at different time of corrosion. Radial distribution functions (RDF) around Fe and Cr atoms were obtained by Fourier transformation of the XAFS spectra. Iron atoms are coordinated by 6 oxygen and/or hydroxyl, and form Fe(O,OH)_6 octahedra. These Fe(O,OH)_6 octahedra compose "Fe(O,OH)₆ network" of rust [7, 8].

RDF around Fe showed that only the 1st and 2nd nearest neighboring correlation (Fe-O and Fe-Fe, respectively) were clear at the early stage of corrosion corresponding to Fig.5(a), and that the 3rd and higher nearest neighboring correlation were not clear. However, the 3rd nearest neighboring correlation (Fe-O) was clearly found when the specimen corrodes more than 0.5 year. This shows the evolution of Fe(O,OH)_6 network as the corrosion progresses.

RDF obtained by Cr K-edges XAFS spectra showed that chromium form a different type of Cr(O,OH)_x structure, suggesting chromium atoms occupy different sites from iron atoms in the Fe(O,OH)_6 network structure of the rust.

Ex situ measurements of the rust were also performed for specimens which experienced a longer period of corrosion. Specimens were dried in air and wet again. Wet-dry cycles were repeated up to 31 years, and rusts formed on specimens MS and WS were investigated using the same techniques.

Based on these *in situ* and *ex situ* measurements, evolution of Fe(O,OH)_6 network during corrosion was revealed [7, 8]. This is illustrated in Fig.6, where Fe and Cr are denoted by small and large closed circles, and O are by large open circles.

At the initial stage of corrosion of MS, iron atoms form Fe(O,OH)_6 units in water or in air with moisture, resulting in formation of colloidal rusts (Fig.6, left). Its structure is similar to that of crystalline $\gamma\text{-FeOOH}$.

However, in the case of WS including Cr and Cu, the situation is different. Chromium addition results in formation of Cr(O,OH)_x units having different structures from Fe(O,OH)_6 . Chromium increases the atomic level heterogeneity in the network through occupying different from that of iron, which was not found in MS. It is also expected that the nucleation energy of the Cr(O,OH)_x unit is lower than that of the Fe(O,OH)_6 and that this decreases nucleation energy. These factors result in the different mode of reaction: growth-limited in WS and nucleation-limited in MS.

As the corrosion progresses after about half a year, the Fe(O,OH)_6 network may change from $\gamma\text{-FeOOH}$ like to $\alpha\text{-FeOOH}$ like. Also in this stage, the Cr(O,OH)_x units affect the evolution of Fe(O,OH)_6 network (Fig.6, middle).

Existence of Cr(O,OH)_x units prevents the network growing rapidly through atomic level heterogeneity in the Fe(O,OH)_6 network. It is also suggested Cr(O,OH)_x prevents water and/or oxygen from penetrating into the steel [9].

Different evolution of the Fe(O,OH)_6 network during corrosion between WS and MS result in different morphology of rusts at the final stage. The rust formed in WS is composed of very fine grain size about 5-15 nm in diameter as found by TEM (Fig.6, right). Contrary to this, the rust formed in MS contain grains as large as 100-1000 nm.

It has been shown that the evolution of Fe(O,OH)_6 network is deeply related with the corrosion resistance. The mechanism revealed by *in situ* observation is expected to lead to designing a new type of WS of the future.

4. CONCLUSION

In situ techniques have been developed for observation of reactions at liquid/metal interfaces. (a) Ions and/or colloids in solutions near the interface were successfully investigated by *in situ* XAFS. This was applied to study pitting of stainless steel. The formation of hydrobromo-complex near the interface was found to play an important role.

(b) Change of atomic structures of rust layers formed on steel was investigated by *in* and *ex situ* X-ray scattering. It has been shown that addition of a small amounts of elements change the evolution of "Fe(O,OH)₆ network" during corrosion, resulting in different corrosion resistance.

Acknowledgements

A part of this work was carried out as collaborative research with (1) KEK, Tsukuba, Japan and (2) Prof. Y. Waseda at Tohoku Univ., Sendai, Japan. The author would like to thank Profs. M. Nomura and T. Matsushita at PF for their supports of the synchrotron experiments.

The author would like to thank Prof. Y. Waseda for collaboration and encouragement of the research. Supports and helpful discussions by Drs. M. Hashimoto, M. Hibi and S. Ito at Nippon Steel are greatly appreciated

References

- [1] M. Kimura, M. Kaneko, and N. Ohta, *ISIJ International* **42**, 1398 (2002).
 [2] M. Nomura, *J. Synchrotron Rad.* **5**, 851 (1998).
 [3] M. Nomura and A. Koyama, in *X-ray Absorption Fine Structure*, edited by S. S. Hasnain (Ellis Horwood, London, 1991), p.667.
 [4] M. Kimura and N. Ohta, *PF Activity Report* 2002 **20**, (2003).
 [5] H. S. Isaacs, J. H. Cho, M. L. Rivers, et al., *J. Electrochem. Soc.* **142**, 1111 (1995).
 [6] H. S. Isaacs and M. Kaneko, in *Inter. Symp. on Pits and Pores* (ECS, Montreal, 1997), p.341.
 [7] M. Kimura, T. Suzuki, G. Sigesato, et al., *J. Japan Inst. Metals* **66**, 166 (2002).
 [8] M. Kimura, T. Suzuki, H. Shigesato, et al., *ISIJ International* **42**, 1534 (2002).
 [9] M. Yamashita, H. Sachi, H. Nagano, et al., *Tetsu to Hagane (ISIJ)* **83**, 448 (1997).

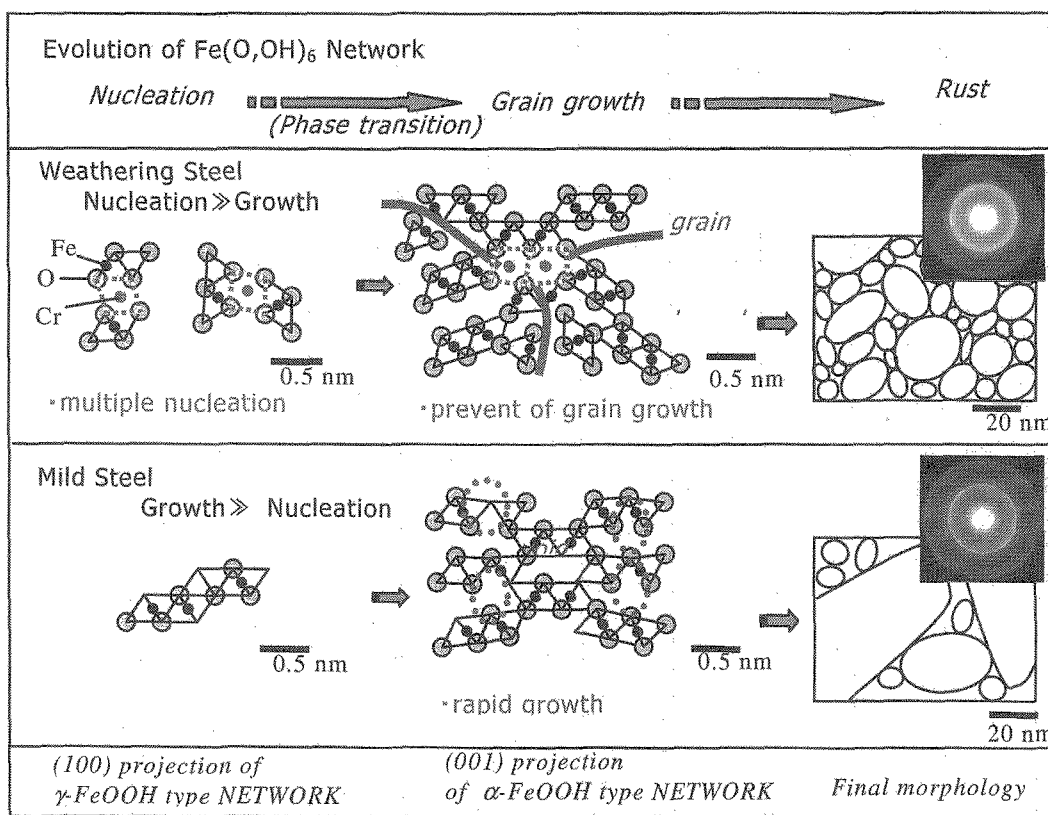


Fig.6 Schematic diagram of the evolution of the $\text{Fe}(\text{O},\text{OH})_6$ network in WS (above) and MS (below) during corrosion.

(Received August 1, 2003; Accepted August 21, 2003)